Departures from local interfacial equilibrium during metal oxidation

Rohit Ramanathan ⬤ and Peter W. Voorhees[*]

Department of Materials Science and Engineering, Northwestern University, Evanston, Illinois, 60208, USA

We use irreversible thermodynamics to formulate a model for the formation of a cation-deficient, *p*-type oxide on the surface of a pure metal in which local equilibrium is not necessarily maintained at the oxide interfaces and no *a priori* assumption regarding a rate limiting step is made. The dissipation rate derived here accounts for most of the conceivable processes that can occur during the oxidation of a metal, including bulk diffusion of cations and surface diffusion along the metal-oxide and gas-oxide interfaces. By including capillary effects in the formulation, shape changes in the oxide, which are usually neglected in most theories, can be described. We examine the steady-state solution of the model in one dimension for planar interfaces, and show that the growth law naturally captures the transition from linear to parabolic kinetics as the film thickens. A characteristic lengthscale for the transition is derived and can be obtained from oxide growth curves as a fitting parameter. Wagner's classical oxidation model is obtained as a limiting case of our more general model. We obtain expressions for the interfacial defect concentrations as a function of the departure from local equilibrium at the interfaces. From these expressions, we show that the exponent for the oxygen pressure dependence of the cation vacancy concentration can deviate from the usual values obtained from equilibrium considerations, and thus measuring nonstandard exponents can indicate a nonequilibrium effect. Our analysis serves to clarify the meaning and validity of the local equilibrium assumption in the context of metal oxidation.

I. INTRODUCTION

When most pure metals are in contact with O_2 at high temperatures, a heterogeneous reaction occurs resulting in the formation of a thin oxide scale on the surface of the metal. The reaction continues and the scale thickens due to transport of either metal or oxygen (sometimes both) across the scale to the reactant at the opposing oxide interface [1]. Growth of the oxide is modelled by formulating appropriately constrained equations for reactant transport in the oxide, with boundary conditions related to the state of the reactions occurring at the metal-oxide and gas-oxide interfaces [2].

It is frequently assumed that equilibrium is established locally at the metal-oxide and gas-oxide interfaces during oxidation [3]. Wagner assumes this to be true in his frequently cited model of metal oxidation [4], and many extensions of that model have maintained this assumption [5–8]. When local interfacial equilibrium is established, the chemical potentials of the reacting species are continuous across the interface and maintain a fixed value that is independent of time [9]. As a result, reactant diffusion across the film is the rate-limiting step [1]. Since the steady-state reactant flux is inversely proportional to the film thickness, L, the film grows according to the parabolic rate law

$$L^2 = k_p t,$$

where k_p is known as the parabolic rate constant, and is typically a function of the driving force for oxidation [1,2].

Parabolic kinetics are observed for large oxide thicknesses where reactant diffusion must be the rate-limiting step.

When the oxide film is thin, the reactant fluxes can be very large and a deviation from local equilibrium, manifesting as a jump discontinuity in the chemical potential at the interface, is expected [9,10]. In this case, the oxidation rate is said to be "interface controlled" and the oxide thickness increases linearly in time. The rate law transitions from linear to parabolic as the oxide thickens [11,12].

For the case of interface control, the boundary conditions are frequently chemical rate laws for the reactions that are presumed to be occurring at the oxide interfaces [13]. Wagner considered the possibility that the linear rate law is due to a deviation from local equilibrium at the gas-oxide interface when the gas-oxide interface reaction becomes rate limiting [14]. Others considered that the reaction control of oxidation occurs while the metal-oxide interface maintains a state of local equilibrium [15]. This requires fast diffusion across the metal-oxide interface such that the vacancy concentration maintains its equilibrium value. Since diffusion in oxides is generally slow and there are various structural complications associated with accommodating a flux across a solid-solid interface, it is difficult to envisage local equilibrium being truly maintained at the metal-oxide interface at all times, particularly during the initial stages of oxide growth [3]. The purpose of this paper is to relax the assumption of local interfacial equilibrium and formulate a general oxidation model in which no *a priori* assumption regarding a rate limiting step is made. We accomplish this by utilizing irreversible thermodynamics to rigorously analyze mass transport in the metal-oxide-gas system. Specifically, we consider the formation of a

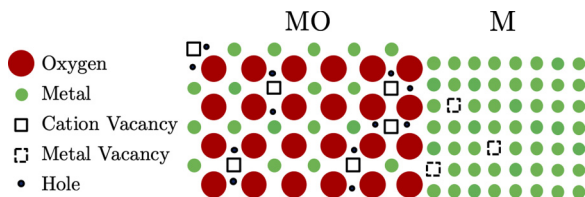———————
[*]p-voorhees@northwestern.edu

FIG. 1. Defect structures of the metal and oxide. The metal contains metal atoms and vacancies, while the oxide contains cations, oxygen ions, cation vacancies, and holes. The oxygen sublattice is assumed to be perfect such that oxygen diffusion is negligible.

cation-deficient, p-type semiconducting oxide MO on the surface of a pure metal M in a pure O_2 atmosphere. The result of the analysis is the set of governing equations and boundary conditions needed for modeling the oxidation transformation in which local equilibrium is not necessarily established at either of the oxide interfaces. Although we focus on oxidation in one dimension with planar interfaces, capillary effects are included in the boundary conditions of the model which enables a self-consistent description of shape changes in oxide due to both bulk and surface diffusion. Capillary effects have generally been neglected to date as most models focus on oxidation in one dimension. The model presented here was derived using the formalism for creep deformation developed by Mishin *et al.* [16]. The present development serves to clarify the meaning and validity of the local equilibrium assumption, and establishes the framework needed to explain recent experiments on "nonequilibrium solute capture," in which metastable oxide solid solutions formed during the oxidation of single phase alloys [17]. This process requires a departure from equilibrium at the metal-oxide interface.

II. THERMODYNAMICS

The crystalline nature of the metal and oxide means that we must consider the presence of the both lattice and electronic defects to formulate a complete thermodynamic description of these phases. The defect structures of the metal and oxide are depicted in Fig. 1. The metal is composed of metal atoms (M) and vacancies (V_M). The oxide has the rocksalt crystal structure and is composed of cations ($M_M^\times$), cation vacancies (V_M''), holes ($h^\bullet$) and oxygen ions ($O_O^\times$). We will assume that holes do not occupy any particular site in the oxide. We use Kröger-Vink notation to denote the structural elements of the oxide which are distinct from thermodynamic components. At all points, we will assume that the metal and oxide phases are completely free of stress.

A. Metal phase

We will assume that the metal is semi-infinite such that transport processes do not lead to changes in the total number of metal lattice sites. The differential Helmholtz free energy of the metal takes the form

$$df_v^M = -sdT + \mu_M d\rho_M + \mu_{V_M} d\rho_{V_M}, \qquad (1)$$

where f_v^M is the Helmholtz free energy per unit volume, s is the entropy per unit volume, and ρ_M and ρ_{V_M} are the concentrations ([mol/m^3]) of these species. Since metal and atoms

occupy the same lattice

$$d\rho_{V_M} = -d\rho_M, \qquad (2)$$

which transforms Eq. (1) to

$$df_v^M = -sdT + \tilde{\mu}_M d\rho_M. \qquad (3)$$

Here, $\tilde{\mu}_M = \mu_M - \mu_{V_M}$ is the diffusion potential of metal atoms with respect to vacancies. Under the isothermal, stress free conditions we consider $f_v^M = \tilde{\mu}_M \rho_M$.

B. Oxide phase

The thermodynamic description of the oxide phase is slightly more complex than that of the metal owing to the presence of electronic defect in addition to a lattice defect, distinct cation and oxygen sublattices, and the presence of an electrostatic constraint. To complete the thermodynamic description of the oxide, it is helpful to consider the idea of building units of the oxides as described in Chapter 2 of Schmalzried [2] and also Lankhorst *et al.* [18]. The idea of building units is to consider the reactions that give the equilibria between the oxide crystal and gaseous metal and oxygen that represent the pure thermodynamic components whose chemical potentials are unambiguously defined. Consideration of these reactions leads to the groups of structural units in the oxide that are thermodynamically relevant.

The reaction that describes the equilibrium between a gaseous metal (denoted g) and the oxide is

$$M(g) + V_M'' + 2h^\bullet \leftrightarrow M_M^\times. \qquad (4)$$
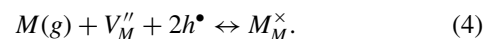
We can rearrange this equation to find that
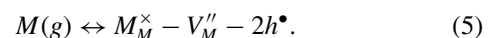
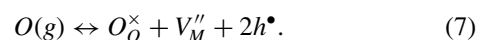$$M(g) \leftrightarrow M_M^\times - V_M'' - 2h^\bullet. \qquad (5)$$

Equilibrium of this reaction is given by the following relation:

$$\mu_{M(g)} = \mu_{M_M^\times} - \mu_{V_M''} - 2\mu_{h^\bullet} = \tilde{\mu}_{M_M^\times}, \qquad (6)$$

where $\tilde{\mu}_{M_M^\times} = \mu_{M_M^\times} - \mu_{V_M''} - 2\mu_{h^\bullet}$. $\tilde{\mu}_{M_M^\times}$ is the only relevant potential for metal in the oxide, and is also a diffusion potential similar to $\tilde{\mu}_M$. The only difference is that holes are included in $\tilde{\mu}_{M_M^\times}$ to balance charge in the oxide. In Eq. (6), the chemical potentials $\mu_{V_M''}$ and $\mu_{h^\bullet}$ could have been written as electrochemical potentials $\bar{\mu}_{V_M''}$ and $\bar{\mu}_{h^\bullet}$ since these are charged species and there is an electrostatic contribution to those chemical potentials. However, upon decomposing the electrochemical potential using the usual convention of $\bar{\mu}_i = \mu_i + z_i \mathcal{F}\phi$, where z_i is the charge number, $\mathcal{F}$ is Faraday's constant, and ϕ is the electrostatic potential in the oxide, we find that the electrostatic contributions from the vacancies and holes cancel, and the diffusion potential $\tilde{\mu}_{M_M^\times}$ in the oxide is just a function of the chemical potentials of the individual structure elements.

The reaction that describes the equilibrium between gaseous atomic oxygen and the oxide is

$$O(g) \leftrightarrow O_O^\times + V_M'' + 2h^\bullet. \qquad (7)$$

This reaction describes the exchange of the oxygen between the gas and the surface of the oxide, which results in the creation of lattice sites in the oxide. An analogous exchange for oxygen in the bulk is not possible since we assume that

there are no oxygen vacancies in the oxide. Equilibrium of this reaction is given by the following relation:

$$\mu_{O(g)} = \mu_{O_O^\times} + \mu_{V_M''} + 2\mu_{h^\bullet} = \tilde{\mu}_{O_O^\times}. \tag{8}$$

Here $\tilde{\mu}_{O_O^\times}$ is the only relevant potential for oxygen in the oxide, and strictly speaking is only defined at the oxide's surface. The interpretation of $\tilde{\mu}_{O_O^\times}$ is different than that of $\tilde{\mu}_{M_M^\times}$ in that $\tilde{\mu}_{O_O^\times}$ is not a diffusion potential. Instead, it a potential that accounts the creation of lattice sites at the oxide surface by forming a pair of a oxygen on an oxygen site together with a vacant cation site and two holes needed to maintain the rocksalt structure and valence neutrality. In Eq. (8), we could have used electrochemical potentials, but as with Eq. (6), the electrostatic contributions from the vacancies and holes cancel, leaving only the regular chemical potentials as part of $\tilde{\mu}_{O_O^\times}$.

We could have proceeded in an analogous fashion as the metal to derive the relevant metal and oxygen potentials in the oxide, but believe that the building unit description is more transparent and makes the distinction between bulk and surface processes more apparent. The structural constraint on the cation sublattice

$$d\rho_{V_M''} = -d\rho_{M_M^\times} \tag{9}$$

and the constraint of charge neutrality

$$d\rho_{h^\bullet} = 2d\rho_{V_M''} \tag{10}$$

are indeed satisfied by the reactions and thus by $\tilde{\mu}_{M_M^\times}$ and $\tilde{\mu}_{O_O^\times}$. Our use of the potentials $\tilde{\mu}_{M_M^\times}$ and $\tilde{\mu}_{O_O^\times}$ conforms with the idea that the chemical potentials of the individual structural elements themselves have no physical meaning and only groups of structural element potentials have physical meaning [2,18].

Since $\tilde{\mu}_{O_O^\times}$ is only defined at the oxide surface, a full description of the Helmholtz free energy of the oxide is only possible at the surface. Here, the following equation holds:

$$df_v^O = -sdT + \tilde{\mu}_{M_M^\times}d\rho_{M_M^\times} + \tilde{\mu}_{O_O^\times}d\rho_{O_O^\times}. \tag{11}$$

This equation implies that under isothermal conditions, the Helmholtz free energy at the surface is

$$f_v^O = \tilde{\mu}_{M_M^\times}\rho_{M_M^\times} + \tilde{\mu}_{O_O^\times}\rho_{O_O^\times}. \tag{12}$$

There is one last thermodynamic relation that is obeyed at the surface which is, using Eqs. (6) and (8):

$$\tilde{\mu}_{M_M^\times} + \tilde{\mu}_{O_O^\times} = \mu_{M_M^\times} + \mu_{O_O^\times} = \mu_{MO}^\circ. \tag{13}$$

Here μ_{MO}° is the chemical potential of an MO formula unit composed of a cation and oxygen ion, and importantly is the pure oxide that contains no defects. We will assume that Eq. (13) holds always, which ultimately means that we are assuming small vacancy concentrations in the oxide at all times.

C. Gas phase

We consider that the gas phase is a uniform atmosphere of O_2. The differential Helmholtz free energy of the gas-phase is

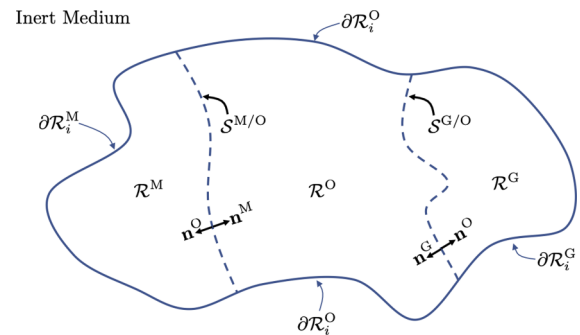$$df_v^G = -sdT + \mu_{O_2}d\rho_{O_2}, \tag{14}$$

FIG. 2. Schematic of the system with the metal, oxide, and gas phases brought into contact with each other. The boundaries and normal orientations are clearly marked.

where f_v^G is the Helmholtz free energy per unit volume in the gas. Under isothermal conditions, this implies that

$$f_v^G = \mu_{O_2}\rho_{O_2}. \tag{15}$$

To simplify the oxygen mass balance at the gas-oxide interface, we will consider the gas phase as composed of oxygen atoms in which the following relations hold:

$$\rho_O = 2\rho_{O_2}, \quad \mu_O = \tfrac{1}{2}\mu_{O_2} \tag{16}$$

so that

$$f_v^G = \mu_O\rho_O. \tag{17}$$

Equations (15) and (17) give the same Helmholtz free energy density.

III. FREE ENERGY DISSIPATION IN THE THREE-PHASE SYSTEM

We now consider the entire system composed of the metal, oxide, and gas and examine the free energy dissipation in each phase as well as well as the dissipation at the metal-oxide and gas-oxide interfaces. The setup for the analysis is depicted in Fig. 2. We embed the entire system in an inert medium to enforce zero-flux boundary conditions away from the interfaces. The metal, oxide, and gas phase occupy the regions $\mathcal{R}^M$, $\mathcal{R}^O$, and $\mathcal{R}^G$ which are bounded by the surfaces $\partial\mathcal{R}^M$, $\partial\mathcal{R}^O$, and $\partial\mathcal{R}^G$. The boundary of the metal can be decomposed as $\partial\mathcal{R}^M = \partial\mathcal{R}_i^M + \mathcal{S}^{M/O}$, where $\partial\mathcal{R}_i^M$ is the portion of $\partial\mathcal{R}^M$ in contact with the inert medium and $\mathcal{S}^{M/O}$ is the portion of the boundary coinciding with the metal-oxide interface. The boundaries $\partial\mathcal{R}^O$ and $\partial\mathcal{R}^G$ can be decomposed similarly, where $\mathcal{S}^{G/O}$ is the surface coinciding with the gas-oxide interface. We use outward pointing normal vectors $\mathbf{n}^M$, $\mathbf{n}^O$, and $\mathbf{n}^G$ for each phase. Along $\mathcal{S}^{M/O}$, $\mathbf{n}^O = -\mathbf{n}^M$, and along $\mathcal{S}^{G/O}$, $\mathbf{n}^O = -\mathbf{n}^G$. Velocities of the phase boundaries are denoted as $\mathbf{v}^M$, $\mathbf{v}^O$, and $\mathbf{v}^G$ for the metal, oxide, and gas phases, respectively.

The reference frame we use for the fluxes is that established by the defect-free, immobile lattice of oxygen ions in the oxide. Because these ions do not move, the metal-oxide interface, which is marked by the terminal surface of oxygen ions, is stationary [17] but can still have a flux across it. As a result $\mathbf{v}^M \cdot \mathbf{n}^M = \mathbf{v}^O \cdot \mathbf{n}^O = 0$ along $\mathcal{S}^{M/O}$. The same is not true along $\mathcal{S}^{G/O}$ since that interface moves as a result

of the addition of oxygen atoms to the oxide surface from the gas-phase. Accordingly, $\mathbf{v}^O = \mathbf{v}^G$ along $\mathcal{S}^{G/O}$ so that the oxide and gas phases are in contact at all times. In principle, the portions of the metal and gas phases, $\partial \mathcal{R}_i^M$ and $\partial \mathcal{R}_i^G$ that are in contact with the inert can move if these phases are finite in extent. Such motion would correspond to shrinking of the metal phase as it oxidizes, in addition to shrinking of the gas phase as it is consumed. For sufficiently large metal and gas phases, the velocities of these boundaries would be very small and negligibly contribute to the dissipation rate we are concerned with here. As such, we take the velocities of the the boundaries $\partial \mathcal{R}_i^M = \partial \mathcal{R}_i^G = 0$. In deriving the dissipation rate in each phase, we will use the local mass conservation equation

$$\frac{\partial \rho_i}{\partial t} = -\nabla \cdot \mathbf{J}_i^L, \tag{18}$$

where $\mathbf{J}_i^L$ is the lattice (or bulk) flux of species i.

A. Dissipation in the metal

The total free energy of the metal is

$$\Phi^M = \int_{\mathcal{R}^M} f_v^M dv. \tag{19}$$

The rate of the free energy change in the metal is

$$\dot{\Phi}^M = -\int_{\mathcal{R}^M} \tilde{\mu}_M \nabla \cdot \mathbf{J}_M^L dv + \int_{\partial \mathcal{R}^M} f_v^M \mathbf{v}^M \cdot \mathbf{n}^M dA. \tag{20}$$

In Eq. (20), the first term corresponds to dissipation of energy by diffusion of metal, and the second terms corresponds to dissipation by the creation or annihilation of metal lattice sites at the the boundary with velocity $\mathbf{v}^M$. Since $\partial \mathcal{R}^M$ is in contact with either the inert medium or the stationary metal-oxide interface $\mathbf{v}^M \cdot \mathbf{n}^M = 0$ along ∂R^M, the metal phase does not change size, and the second term is 0. Applying the product rule for divergences, we can transform Eq. (20) into the following form:

$$\dot{\Phi}^M = \int_{\mathcal{R}^M} \nabla \tilde{\mu}_M \cdot \mathbf{J}_M^L dv - \int_{\mathcal{R}^M} \nabla \cdot (\tilde{\mu}_M \mathbf{J}_M^L) dv. \tag{21}$$

We then apply the divergence theorem to the second term to arrive at the following equation for the free energy dissipation rate of the metal phase:

$$\dot{\Phi}^M = \int_{\mathcal{R}^M} \nabla \tilde{\mu}_M \cdot \mathbf{J}_M^L dv - \int_{\partial \mathcal{R}^M} \tilde{\mu}_M \mathbf{J}_M^L \cdot \mathbf{n}^M dA. \tag{22}$$

B. Dissipation in the oxide

The oxide is a growing phase and we assign to $\mathbf{v}^O$ the velocity of the boundary $\partial \mathcal{R}^O$. Similarly to the metal, $\mathbf{v}^O = 0$ along $\mathcal{S}^{M/O}$ and $\partial \mathcal{R}_i^O$ and is only nonzero along $\mathcal{S}^{G/O}$ which the interface where growth of rocksalt oxides occurs [3]. The total free energy of the oxide is

$$\Phi^O = \int_{\mathcal{R}^O} f_v^O dv. \tag{23}$$

The rate of free energy dissipation in the oxide is

$$\dot{\Phi}^O = -\int_{\mathcal{R}^O} \left(\tilde{\mu}_{M_M^\times} \nabla \cdot \mathbf{J}_{M_M^\times}^L + \tilde{\mu}_{O_O^\times} \nabla \cdot \mathbf{J}_{O_O^\times}^L \right) dv$$
$$+ \int_{\mathcal{S}^{G/O}} f_v^O \mathbf{v}^O \cdot \mathbf{n}^O dA. \tag{24}$$

In Eq. (24), $\mathbf{J}_{O_O^\times}^L = 0$ because bulk fluxes of oxygen are prohibited by the lack of oxygen vacancies. The second integral in Eq. (24) represents the free energy dissipated by growth of the oxide and addition of lattice sites at the oxide surface. We can now apply the product rule for divergences and the divergence theorem to Eq. (24) to obtain the following equation for the free energy dissipation in the oxide:

$$\dot{\Phi}^O = \int_{\partial \mathcal{R}^O} \nabla \tilde{\mu}_{M_M^\times} \cdot \mathbf{J}_{M_M^\times}^L dv - \int_{\partial \mathcal{R}^O} \tilde{\mu}_{M_M^\times} \mathbf{J}_{M_M^\times}^L \cdot \mathbf{n}^O dA$$
$$+ \int_{\mathcal{S}^{G/O}} f_v^O \mathbf{v}^O \cdot \mathbf{n}^O dA. \tag{25}$$

C. Dissipation in the gas

We treat the gas as an oxygen atmosphere with uniform pressure. As the oxide grows, the gas phase shrinks with velocity $\mathbf{v}^G$. Note that $\mathbf{v}^G$ is nonzero only along the gas-oxide interface $\mathcal{S}^{G/O}$. The total free energy of the gas is

$$\Phi^G = \int_{\mathcal{R}^M} f_v^G dv. \tag{26}$$

The rate of change of the gas free energy is

$$\dot{\Phi}^G = -\int_{\mathcal{R}^G} \mu_O \nabla \cdot \mathbf{J}_O^L dv + \int_{\mathcal{S}^{G/O}} f_v^G \mathbf{v}^G \cdot \mathbf{n}^G dA. \tag{27}$$

Since the gas has uniform pressure, $\mathbf{J}_O^L = 0$ and

$$\dot{\Phi}^G = \int_{\mathcal{S}^{G/O}} f_v^G \mathbf{v}^G \cdot \mathbf{n}^G dA. \tag{28}$$

D. Dissipation at the interfaces

The total energy of the system depicted in Fig. 2 is given by the equation

$$\Phi = \Phi^M + \Phi^O + \Phi^G + \Phi^{M/O} + \Phi^{G/O}. \tag{29}$$

Here, $\Phi^{M/O}$ and $\Phi^{G/O}$ give the free energy of the metal-oxide and gas-oxide interface, i.e.,

$$\Phi^{M/O} = \int_{\mathcal{S}^{M/O}} \gamma^{M/O} dA, \ \ \Phi^{G/O} = \int_{\mathcal{S}^{G/O}} \gamma^{G/O} dA, \tag{30}$$

where $\gamma^{M/O}$ and $\gamma^{G/O}$ are the interfacial energies of the metal-oxide and gas-oxide interfaces. We have previously derived the equations for the rates of free energy dissipation in the metal, oxide, and gas and now turn to the rate of free energy dissipation at the interfaces. We will assume that the interfacial energies are isotropic and thus

$$\gamma^{M/O} = \gamma^{M/O}(T), \ \ \gamma^{G/O} = \gamma^{G/O}(T). \tag{31}$$

This means that faceting or anisotropic energy of the oxide surface is not described but could be added in the future.

The dissipation rates at the interfaces have the form

$$\dot{\Phi}^{M/O} = \int_{\mathcal{S}^{M/O}} \dot{\gamma}^{M/O} dA + \int_{\mathcal{S}^{M/O}} \gamma^{M/O} d\dot{A}, \qquad (32)$$

$$\dot{\Phi}^{G/O} = \int_{\mathcal{S}^{G/O}} \dot{\gamma}^{G/O} dA + \int_{\mathcal{S}^{G/O}} \gamma^{G/O} d\dot{A}. \qquad (33)$$

By Eq. (31), $\dot{\gamma}^{M/O} = \dot{\gamma}^{G/O} = 0$, and the first integrals in Eqs. (32) and (33) are 0. The rates of changes of the interfacial areas are given by

$$d\dot{A} = \kappa \mathbf{v} \cdot \mathbf{n} dA, \qquad (34)$$

where κ gives the curvature of the interface and is defined as $\kappa = \nabla \cdot \mathbf{n}$. Note that this definition of κ gives the correct sign of the curvature for the outward pointing normal vectors $\mathbf{n}^O$ of the oxide. Since $\mathbf{n}^M$ and $\mathbf{n}^G$ point in opposite directions to $\mathbf{n}^O$ along $\mathcal{S}^{M/O}$ and $\mathcal{S}^{G/O}$, the curvatures of these two interfaces have opposite signs when defined with respect to the metal and gas phases.

Using this, we find that

$$\dot{\Phi}^{M/O} = 0, \qquad (35)$$

$$\dot{\Phi}^{G/O} = \int_{\mathcal{S}^{G/O}} \gamma^{G/O} \kappa^O \mathbf{v}^O \cdot \mathbf{n}^O dA. \qquad (36)$$

For Eq. (35), we used the fact that $\mathbf{v}^O \cdot \mathbf{n}^O = 0$ along $\mathcal{S}^{M/O}$.

E. Total free energy dissipation

The total rate of free energy dissipation for the system is

$$\dot{\Phi} = \int_{\mathcal{R}^M} \nabla \tilde{\mu}_M \cdot \mathbf{J}_M^L dv + \int_{\mathcal{R}^O} \nabla \tilde{\mu}_{M_M^\times} \cdot \mathbf{J}_{M_M^\times}^L dv$$

$$- \int_{\partial \mathcal{R}^M} \tilde{\mu}_M \mathbf{J}_M^L \cdot \mathbf{n}^M dA - \int_{\partial \mathcal{R}^O} \tilde{\mu}_{M_M^\times} \mathbf{J}_{M_M^\times}^L \cdot \mathbf{n}^O dA$$

$$+ \int_{\mathcal{S}^{G/O}} f_v^O \mathbf{v}^O \cdot \mathbf{n}^O dA + \int_{\partial \mathcal{S}^{G/O}} f_v^G \mathbf{v}^G \cdot \mathbf{n}^G dA$$

$$+ \int_{\mathcal{S}^{G/O}} \gamma^{G/O} \kappa^O \mathbf{v}^O \cdot \mathbf{n}^O dA. \qquad (37)$$

We now turn to the evaluation of the surface integrals along $\partial \mathcal{R}^M$, $\partial \mathcal{R}^O$, and $\partial \mathcal{R}^G$. For the integral along $\partial \mathcal{R}^M$ we have

$$\int_{\partial \mathcal{R}^M} \tilde{\mu}_M \mathbf{J}_M^L \cdot \mathbf{n}^M dA = \int_{\mathcal{S}^{M/O}} \tilde{\mu}_M \mathbf{J}_M^L \cdot \mathbf{n}^M dA. \qquad (38)$$

Here, we used that fact that the normal flux of metal along $\partial \mathcal{R}_i^M$ must vanish since the inert medium is incapable of taking in metal atoms. Similar arguments are used to simplify the remaining surface integrals to just terms involving the interfaces. Doing this, we find that the total rate of free energy dissipation is

$$\dot{\Phi} = \int_{\mathcal{R}^M} \nabla \tilde{\mu}_M \cdot \mathbf{J}_M^L dv + \int_{\mathcal{R}^O} \nabla \tilde{\mu}_{M_M^\times} \cdot \mathbf{J}_{M_M^\times}^L dv$$

$$- \int_{\mathcal{S}^{M/O}} \tilde{\mu}_M \mathbf{J}_M^L \cdot \mathbf{n}^M dA - \int_{\mathcal{S}^{M/O}} \tilde{\mu}_{M_M^\times} \mathbf{J}_{M_M^\times}^L \cdot \mathbf{n}^O dA$$

$$- \int_{\mathcal{S}^{G/O}} \tilde{\mu}_{M_M^\times} \mathbf{J}_{M_M^\times}^L \cdot \mathbf{n}^O + \int_{\mathcal{S}^{G/O}} f_v^O \mathbf{v}^O \cdot \mathbf{n}^O dA$$

$$+ \int_{\mathcal{S}^{G/O}} f_v^G \mathbf{v}^G \cdot \mathbf{n}^G dA + \int_{\mathcal{S}^{G/O}} \gamma^{G/O} \kappa^O \mathbf{v}^O \cdot \mathbf{n}^O dA. \quad (39)$$

F. Mass conservation

Equation (39), as written, does not account for the exchanges of mass between the metal and oxide and the gas and the oxide which result in growth. We now transform the integrals at the metal-oxide and gas-oxide interfaces in a manner that obeys mass conservation by introducing the following terms:

$$j_M^M = -\mathbf{J}_M^L \cdot \mathbf{n}^M, \qquad (40)$$

$$j_M^O = -\mathbf{J}_{M_M^\times}^L \cdot \mathbf{n}^O, \qquad (41)$$

$$\left(j_M^M + j_M^O \right) = -\nabla_s \cdot \mathbf{J}_M^s. \qquad (42)$$

Here, j_M^M and j_M^O represent the number of metal atoms per unit area per unit time that enter the metal and oxide phases, respectively, from the metal-oxide interface. Equation (42) represents the conservation condition that the total number atoms that enter each phase is equal to the surface divergence of the surface diffusion flux $\mathbf{J}_M^s$. In the absence of diffusion along the interface, we find that $j_M^M = -j_M^O$ as expected. Equations (40) and (41) allow us to combine the two integrals at the metal oxide interface as

$$- \int_{\mathcal{S}^{M/O}} \left(\tilde{\mu}_M \mathbf{J}_M^L \cdot \mathbf{n}^M + \tilde{\mu}_{M_M^\times} \mathbf{J}_{M_M^\times}^L \cdot \mathbf{n}^O \right) dA$$

$$= \int_{\mathcal{S}^{M/O}} \left(\tilde{\mu}_M j_M^M + \tilde{\mu}_M j_M^O \right) dA. \qquad (43)$$

The conservation of atoms at the gas-oxide interface is captured by the equations

$$\mathbf{J}_{M_M^\times}^L \cdot \mathbf{n}^O = \rho_{M_M^\times} \mathbf{v}^O \cdot \mathbf{n}^O, \qquad (44)$$

$$j_O^O = \rho_{O_O^\times} \mathbf{v}^O \cdot \mathbf{n}^O, \qquad (45)$$

$$j_O^G = \rho_O \mathbf{v}^G \cdot \mathbf{n}^G, \qquad (46)$$

$$\left(j_O^O + j_O^G \right) = -\nabla_s \cdot \mathbf{J}_O^s. \qquad (47)$$

Here j_O^O and j_O^G are defined analogously to j_M^M and j_M^O, and $\mathbf{J}_O^s$ is the surface diffusion flux of oxygen.

Utilizing Eq. (44), the first two integrals at the gas-oxide interface in Eq. (39) are combined to give the term

$$\int_{\mathcal{S}^{G/O}} \left(f_v^O - \tilde{\mu}_{M_M^\times} \rho_{M_M^\times} \right) \mathbf{v}^O \cdot \mathbf{n}^O dA = \int_{\mathcal{S}^{G/O}} \tilde{\mu}_{O_O^\times} \rho_{O_O^\times} \mathbf{v}^O \cdot \mathbf{n}^O dA. \qquad (48)$$

Using Eq. (45), we eliminate the velocity of the interface in Eq. (48) to obtain

$$\int_{\mathcal{S}^{G/O}} \tilde{\mu}_{O_O^\times} \rho_{O_O^\times} \mathbf{v}^O \cdot \mathbf{n}^O dA = \int_{\mathcal{S}^{G/O}} \tilde{\mu}_{O_O^\times} j_O^O dA. \qquad (49)$$

We then apply Eq. (46) to the third integral at the gas-oxide interface in Eq. (39) to show

$$\int_{\mathcal{S}^{G/O}} f_v^G \mathbf{v}^G \cdot \mathbf{n}^G dA = \int_{\mathcal{S}^{G/O}} \frac{f_v^G}{\rho_O} j_O^G dA = \int_{\mathcal{S}^{G/O}} \mu_O j_O^G dA. \qquad (50)$$

Finally, for the last integral of Eq. (39), we can use Eq. (45) to eliminate the interface velocity and find

$$\int_{\mathcal{S}^{G/O}} \gamma^{G/O} \kappa^O \mathbf{v}^O \cdot \mathbf{n}^O dA$$
$$= \int_{\mathcal{S}^{G/O}} \Omega^O \gamma^{G/O} \kappa^O j_O^O dA. \tag{51}$$

Here, $\Omega^O = 1/\rho_{O_O^\times}$ is the volume per oxygen ion in the oxide, which is roughly equivalent to the volume of an MO formula unit due to the large size discrepancy between the oxygen ions and cations in the oxides, with the cations usually being much smaller [2]. Putting everything together, the dissipation rate becomes

$$\dot{\Phi} = \int_{\mathcal{R}^M} \nabla \tilde{\mu}_M \cdot \mathbf{J}_M^L dv + \int_{\mathcal{R}^O} \nabla \tilde{\mu}_{M_M^\times} \cdot \mathbf{J}_{M_M^\times}^L dv$$
$$+ \int_{\mathcal{S}^{M/O}} (\tilde{\mu}_M j_M^M + \tilde{\mu}_{M_M^\times} j_M^O) dA$$
$$+ \int_{\mathcal{S}^{G/O}} (\hat{\mu}_{O_O^\times} j_O^O + \mu_O j_O^G) dA. \tag{52}$$

In Eq. (52), $\hat{\mu}_{O_O^\times} = \tilde{\mu}_{O_O^\times} + \Omega^O \gamma^{G/O} \kappa^O$, and is the effective chemical potential of oxygen with the interfacial energy contribution included.

IV. EQUILIBRIUM CONDITIONS AND TRANSPORT EQUATIONS

Equation (52) captures the energy dissipation in the entire system, but is not yet in a form in which the interfacial driving forces are easily identified. To do this it is useful to introduce the following notation and identities:

$$[A]^{M/O} = A^M - A^O, \quad [A]^{G/O} = A^G - A^O, \tag{53}$$

$$\langle A \rangle^{M/O} = \frac{A^M + A^O}{2}, \quad \langle A \rangle^{G/O} = \frac{A^G + A^O}{2}, \tag{54}$$

$$[AB] = \langle A \rangle [B] + [B] \langle A \rangle, \tag{55}$$

$$\langle AB \rangle = \langle A \rangle \langle B \rangle + \frac{1}{4} [A][B]. \tag{56}$$

Using these identities, we can follow the procedure in the Appendix of Mishin *et al.* [16] to cast Eq. (39) into the form

$$\dot{\Phi} = \int_{\mathcal{R}^M} \nabla \tilde{\mu}_M \cdot \mathbf{J}_M^L dv + \int_{\mathcal{R}^O} \nabla \tilde{\mu}_{M_M^\times} \cdot \mathbf{J}_{M_M^\times}^L dv$$
$$+ \int_{\mathcal{S}^{M/O}} \nabla_s \langle \tilde{\mu}_M \rangle^{M/O} \cdot \mathbf{J}_M^s dA - \int_{\mathcal{S}^{M/O}} [\tilde{\mu}_M]^{M/O} j_M^n dA$$
$$+ \int_{\mathcal{S}^{G/O}} \nabla_s \langle \tilde{\mu}_O \rangle^{G/O} \cdot \mathbf{J}_O^s dA - \int_{\mathcal{S}^{G/O}} [\hat{\mu}_O]^{G/O} j_O^n dA. \tag{57}$$

Here j_M^n gives the net flux of metal atoms normal to the metal-oxide interface into the oxide, while j_O^n gives the net flux of atoms normal to the gas-oxide interface into the oxide. Each of the integrals in Eq. (57) gives a force-flux conjugate pair that results in dissipation of energy in the bulk phases and at the interfaces.

Equation (57) is now in a form that allows us to clearly identify the equilibrium conditions. In equilibrium, $\dot{\Phi} = 0$ and

we can treat any flux as a variation in the system [16]. As a result we conclude that in equilibrium

$$\tilde{\mu}_M = \text{const. in } \mathcal{R}^M, \tag{58}$$

$$\tilde{\mu}_{M_M^\times} = \text{const. in } \mathcal{R}^O, \tag{59}$$

$$\langle \tilde{\mu}_M \rangle = \text{const. along } \mathcal{S}^{M/O}, \tag{60}$$

$$[\tilde{\mu}_M]^{M/O} = 0 \text{ along } \mathcal{S}^{M/O}, \tag{61}$$

$$\langle \tilde{\mu}_O \rangle = \text{const. along } \mathcal{S}^{G/O}, \tag{62}$$

$$[\hat{\mu}_O]^{G/O} = 0 \text{ along } \mathcal{S}^{G/O}. \tag{63}$$

Equations (58) to (61) imply that, in equilibrium, the diffusion potential of metal achieves a uniform value in the metal and oxide, and that the values of the diffusion potential in the metal and oxide are equal. Equations (62) and (63) imply that the effective chemical potential of oxygen at the oxide surface is equal to the gas chemical potential. Note that in this case, $[\hat{\mu}_O]$ includes the capillary shift of the oxygen potential and thus applies to a curved interface. The fact that the oxygen potential for our oxide is only defined at the surface means that the oxygen equilibrium condition is confined only to the gas-oxide interface.

Equation (57) also allows to write the phenomenological equations for transport in the bulk phases and across the interfaces. Ignoring cross effects at the interfaces, the transport equations are

$$\mathbf{J}_M^L = -\mathcal{K}_M \nabla \tilde{\mu}_M, \tag{64}$$

$$\mathbf{J}_{M_M^\times}^L = -\mathcal{K}_{M_M^\times} \nabla \tilde{\mu}_{M_M^\times}, \tag{65}$$

$$\mathbf{J}_M^s = -\mathcal{L}_M \nabla \langle \tilde{\mu}_M \rangle^{M/O}, \tag{66}$$

$$\mathbf{J}_O^s = -\mathcal{L}_O \nabla \langle \hat{\mu}_O \rangle^{G/O}, \tag{67}$$

$$j_M^n = \mathcal{M}_M [\tilde{\mu}_M]^{M/O}, \tag{68}$$

$$j_O^s = \mathcal{M}_O [\hat{\mu}_O]^{G/O}. \tag{69}$$

Here, $\mathcal{K}$ is the phenomenological coefficient for bulk diffusion, $\mathcal{L}$ is the coefficient for surface diffusion, $\mathcal{M}$ is the coefficient for the fluxes normal to the interfaces. Each $\mathcal{K}$, $\mathcal{L}$, and $\mathcal{M}$ must be positive to guarantee that the dissipation rate given by Eq. (57) leads to a decrease in the free energy. We consider that the transport coefficients $\mathcal{K}_M$, $\mathcal{K}_{M_M^\times}$, $\mathcal{L}_M$, and $\mathcal{L}_O$ are scalars, which implies isotropic diffusion. The transport coefficients can be interpreted as atomic mobility terms. $\mathcal{K}$ represents a mobility in the bulk, $\mathcal{L}$ represents the mobility *along* the interface, and $\mathcal{M}$ gives the mobility of atoms *across* the interface. To simplify the analysis and obtain analytical solutions that convey the essential ideas of the theory, we will assume that these quantities are independent of composition. The values of $\mathcal{L}$ and $\mathcal{M}$ will strongly depend on the structure of the interface, and thus will expected to depend on the orientations of the interfaces between the phases.

At this point it helpful to provide an alternate interpretation of the normal fluxes j_M^n and j_O^n. If we expand the driving forces

for these fluxes ($[\tilde{\mu}_M]^{M/O}$ and $[\hat{\mu}_O]^{G/O}$) in terms of the virtual chemical potentials of the individual structure elements, we find that they are equivalent to the driving forces for the interfacial reactions

$$M + V_M'' + 2h^\bullet \to M_M^\times + V_M, \ \ \Delta G_{M/O} = -[\tilde{\mu}_M]^{M/O}, \quad (70)$$

$$\tfrac{1}{2}O_2 \to O_O^\times + V_M'' + 2h^\bullet, \ \ \Delta G_{G/O} = -[\hat{\mu}_O]^{G/O} \quad (71)$$

that are occurring at the metal-oxide and gas-oxide interfaces, respectively. Note the ΔG values given in Eqs. (70) and (71) correspond to the driving forces at the interfaces, and do not necessarily sum to the total oxidation driving force. Thus, the fluxes j_M^n and j_O^n, can be thought of as measures of the rates of these reactions, and $\mathcal{M}_M$ and $\mathcal{M}_O$ have an additional interpretation as reaction rate constants. This interpretation is especially interesting considering that reactions are not formally part of the model, but arise naturally from the transport analysis.

We are now in a position to summarize the governing equations and boundary conditions for the growth of oxide. The governing equations are

$$\frac{\partial \rho_M}{\partial t} = -\nabla \cdot \mathbf{J}_M^L \ \text{in} \ \mathcal{R}^M, \quad (72)$$

$$\frac{\partial \rho_{M_M^\times}}{\partial t} = -\nabla \cdot \mathbf{J}_{M_M^\times}^L \ \text{in} \ \mathcal{R}^O. \quad (73)$$

The boundary conditions for the oxide growth problem are the mass conservation conditions at the interfaces discussed earlier. The mass conservation considerations relate the bulk [superscript (L)], surface (superscript O), and normal (superscript O) fluxes at the interfaces at the metal-oxide and gas-oxide interfaces as

$$\mathbf{J}_M^L \cdot \mathbf{n}^M + \mathbf{J}_{M_M^\times}^L \cdot \mathbf{n}^O = -\nabla_s \cdot \mathbf{J}_M^s \ \text{at} \ \mathcal{S}^{M/O}, \quad (74)$$

$$\mathbf{J}_{M_M^\times}^L \cdot \mathbf{n}^O = j_M^n \ \text{at} \ \mathcal{S}^{M/O}, \quad (75)$$

$$\mathbf{J}_{M_M^\times}^L \cdot \mathbf{n}^O = \rho_{M_M^\times}\mathbf{v}^O \cdot \mathbf{n}^O \ \text{at} \ \mathcal{S}^{G/O}, \quad (76)$$

$$\left(\rho_{O_O^\times} - \rho_O\right)\mathbf{v}^O \cdot \mathbf{n}^O = -\nabla_s \cdot \mathbf{J}_O^s \ \text{at} \ \mathcal{S}^{G/O}, \quad (77)$$

$$\rho_{O_O^\times}\mathbf{v}^O \cdot \mathbf{n}^O = j_O^n \ \text{at} \ \mathcal{S}^{G/O}, \quad (78)$$

where the fluxes $\mathbf{J}_M^L$, $\mathbf{J}_{M_M^\times}^L$, $\mathbf{J}_M^s$, $\mathbf{J}_O^s$, j_M^n, and j_O^n are related to the diffusion potentials according to Eqs. (64) to (69).

V. PLANAR INTERFACES

We illustrate the physics contained in this model by considering the case of planar oxide growth in one dimension. While the equations hold for nonplanar interfaces and interfacial diffusion, the analysis for nonplanar geometries is significantly more complex and will not be treated here. We examine the case of planar interfaces, which is the context for which oxidation models have typically been developed and analyzed, and will neglect surface diffusion. For planar interface, $\kappa^O = 0$ and $\hat{\mu}_{O_O^\times} = \tilde{\mu}_{O_O^\times}$. To simplify the analysis and focus our attention on the growing oxide phase, we make a few assumptions about mass transport in the metal and oxide. First, we assume that diffusion in the metal is sufficiently fast
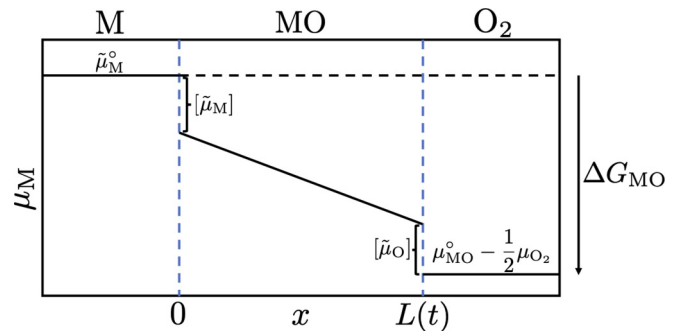

FIG. 3. Depiction of the coordinate system and diffusion potential distribution for the analysis of oxide growth in one dimension.

such that the diffusion potential in the metal at the metal-oxide interface is fixed at its standard state value throughout growth of the oxide, and thus the vacancy concentration in the metal at the metal-oxide interface remains constant. This assumption is reasonable since oxidation experiments on Ni find that vacancies in the oxide do not pile up at the metal-oxide interface and can diffuse long distances in the metal, and that the rate limiting step for oxide growth is diffusion in the oxide, not the metal [3,19].

A. General solution of the model

Using Eq. (65) in Eq. (73) yields a diffusion equation for the concentration of metal ions in the oxide. Similar to most oxidation models [3–6], we will assume that diffusion in the oxide is fast relative the the velocity of the gas-oxide interface such that we can make the quasistationary approximation where $\partial \rho_{M_M^\times}/\partial t \approx 0$ and obtain a linear diffusion potential profile in the oxide of the form

$$\tilde{\mu}_{M_M^\times}(x) = A + Bx. \quad (79)$$

The coordinate system we use is depicted in Fig. 3. The metal-oxide interface is located at the fixed position $x = 0$, while the gas-oxide interface is located at $x = L(t)$. The boundary conditions for the nonequilibrium M/O and G/O interfaces are

$$J_{M_M^\times}^L = \mathcal{M}_M[\tilde{\mu}_M]^{M/O} \ \text{at} \ x = 0, \quad (80)$$

$$J_{M_M^\times}^L = \rho_{M_M^\times}V \ \text{at} \ x = L(t), \quad (81)$$

$$V = \frac{dL}{dt} = \Omega^O j_O^n = \Omega^O \mathcal{M}_O[\tilde{\mu}_O]^{G/O} \ \text{at} \ x = L(t), \quad (82)$$

where we used Eq. (69) to relate the interfacial flux to the jump in the diffusion potential at the G/O interface. We combine Eqs. (81) and (82) to find the new boundary condition

$$J_{M_M^\times}^L = \rho_{M_M^\times}\Omega^O \mathcal{M}_O[\tilde{\mu}_O]^{G/O} \approx \mathcal{M}_O[\tilde{\mu}_O]^{G/O} \ \text{at} \ x = L(t). \quad (83)$$

Applying the two boundary conditions given by Eqs. (80) and (83) to the general solution, we find that jumps in the diffusion

potentials at the the metal-oxide and gas-oxide interfaces are linked as

$$[\tilde{\mu}_M]^{M/O} = \frac{\mathcal{M}_O}{\mathcal{M}_M}[\tilde{\mu}_O]^{G/O}, \tag{84}$$

$$B = -\frac{\mathcal{M}_O}{\mathcal{K}_{M_M^\times}}[\tilde{\mu}_O]^{G/O}, \tag{85}$$

and

$$A = \tilde{\mu}_M^\circ - [\tilde{\mu}_M]^{M/O} = \tilde{\mu}_M^\circ - \frac{\mathcal{M}_O}{\mathcal{M}_M}[\tilde{\mu}_O]^{G/O}, \tag{86}$$

where A is the value of the diffusion potential at the metal-oxide interface. Thus, the cation diffusion potential profile in the oxide is

$$\tilde{\mu}_{M_M^\times}(x) = \tilde{\mu}_M^\circ - \frac{\mathcal{M}_O}{\mathcal{M}_M}[\tilde{\mu}_O]^{G/O} - \frac{\mathcal{M}_O}{\mathcal{K}_{M_M^\times}}[\tilde{\mu}_O]^{G/O}x. \tag{87}$$

Using Eq. (13) we can relate the diffusion potential at the gas-oxide interface to the jump in the oxygen potential as

$$\tilde{\mu}_{M_M^\times}(L) = \mu_{MO}^\circ - \tilde{\mu}_{O_O^\times} = \mu_{MO}^\circ - \mu_O + [\tilde{\mu}_O]^{G/O}. \tag{88}$$

Thus using Eq. (87), we can solve for $[\tilde{\mu}_O]^{G/O}$ as

$$[\tilde{\mu}_O]^{G/O} = -\left(\frac{\mathcal{M}_M\mathcal{K}_{M_M^\times}}{\mathcal{M}_M\mathcal{M}_O L + \mathcal{K}_{M_M^\times}(\mathcal{M}_M + \mathcal{M}_O)}\right)\Delta G_{MO}. \tag{89}$$

By Eq. (84),

$$[\tilde{\mu}_M]^{M/O} = -\left(\frac{\mathcal{M}_O\mathcal{K}_{M_M^\times}}{\mathcal{M}_M\mathcal{M}_O L + \mathcal{K}_{M_M^\times}(\mathcal{M}_M + \mathcal{M}_O)}\right)\Delta G_{MO}. \tag{90}$$

Finally the growth rate of the film is

$$V = \frac{dL}{dt} = -\left(\frac{\Omega^O\mathcal{M}_M\mathcal{M}_O\mathcal{K}_{M_M^\times}}{\mathcal{M}_M\mathcal{M}_O L + \mathcal{K}_{M_M^\times}(\mathcal{M}_M + \mathcal{M}_O)}\right)\Delta G_{MO}. \tag{91}$$

In Eqs. (89) to (91), $\Delta G_{MO} = \mu_{MO}^\circ - \mu_O - \tilde{\mu}_M^\circ = \mu_{MO}^\circ - \frac{1}{2}\mu_{O_2} - \tilde{\mu}_M^\circ$ is the total driving force for the net oxidation reaction $M + \frac{1}{2}O_2 \rightarrow MO + V_M$. In this equation, μ_{MO}°, and μ_{O_2} are taken at the gas-oxide interface (where the oxide forms) and $\tilde{\mu}_M^\circ$ is taken at the metal-oxide interface. For oxide growth, $\Delta G_{MO} < 0$ and the growth rate of the oxide as well as the potential jumps are positive, as expected.

Equations (89) to (91) represent the most important quantities for the nonequilibrium reaction-diffusion problem leading to the formation of the oxide. The prefactors of Eqs. (89) and (90) give the fraction of the total oxidation driving force that is dissipated at the gas-oxide and metal-oxide interfaces, respectively. The remaining portion of the driving force is dissipated by diffusion through the bulk oxide. Dissipation by diffusion is only possible for nonzero diffusion potential gradients in the bulk oxide, which occurs whenever $[\tilde{\mu}_O] + [\tilde{\mu}_M] < \Delta G_{MO}$, as depicted in Fig. 3.

B. Growth kinetics

It is worth further examining the growth law given by Eq. (91). If we divide the numerator and denominator by

$\mathcal{M}_M\mathcal{M}_O$, the growth law is transformed to the more informative form

$$\frac{dL}{dt} = -\left(\frac{\Omega^O\mathcal{K}_{M_M^\times}}{L + L^*}\right)\Delta G_{MO}, \tag{92}$$

where

$$L^* = \frac{\mathcal{K}_{M_M^\times}}{\mathcal{M}_{\text{eff}}}, \tag{93}$$

$$\mathcal{M}_{\text{eff}} = \frac{\mathcal{M}_M\mathcal{M}_O}{\mathcal{M}_M + \mathcal{M}_O}. \tag{94}$$

L^* is a kinetically defined lengthscale in the film that takes into accounts the interplay between interfacial reaction kinetics and bulk diffusion in the oxide. $\mathcal{M}_{\text{eff}}$ is the effective flux coefficient for the two interfacial reactions occurring in series. $\mathcal{M}_{\text{eff}}$ essentially gives the rate constant of the oxidation reaction when both of the interfacial reactions are occurring at a finite rates. In analogy to ambipolar diffusion where the species with the lower mobility determines the ambipolar diffusivity [18], from Eq. (94) we can see that the interfacial reaction with the lower rate constant determines the overall rate of the oxidation reaction. For example, when the mobility of atoms crossing the metal-oxide interface is less than that at the oxide-vapor interface, or, if the oxide-vapor interface is nearly in equilibrium, $\mathcal{M}_M \ll \mathcal{M}_O$, $\mathcal{M}_{\text{eff}} \approx \mathcal{M}_M$.

When $L \ll L^*$

$$\frac{dL}{dt} = -\Omega^O\mathcal{M}_{\text{eff}}\Delta G_{MO} \tag{95}$$

and the oxide grows linearly in time. When $L \gg L^*$, the parabolic rate law is obtained

$$\frac{dL}{dt} = \frac{k_P}{2L}, \tag{96}$$

where $k_P = -2\Omega^O\mathcal{K}_{M_M^\times}\Delta G_{MO}$. The linear growth rate given by Eq. (95) represents the maximum growth rate that is possible in the system, and resolves the issue of the Wagner model's prediction of an unphysical, infinite growth rate when the film thickness goes to zero.

It is possible to determine the kinetic coefficients $\mathcal{K}_{M_M^\times}$ and $\mathcal{M}_{\text{eff}}$ through experiments by carefully measuring the oxide film thickness as a function of time. Integration of Eq. (92) with the initial condition $L(0) = 0$ gives

$$L(t) = -L^* + \sqrt{-2\Omega^O\mathcal{K}_{M_M^\times}\Delta G_{MO}t + L^{*2}}. \tag{97}$$

Since Ω^O is known for most oxides, and ΔG_{MO} can be readily calculated as a function of P_{O_2} using tabulated thermodynamic data, the value of $\mathcal{K}_{M_M^\times}$ and L^* can be obtained by fitting Eq. (97) to oxide thickness vs time data. However, only $\mathcal{M}_{\text{eff}}$ can be determined, the individual coefficients $\mathcal{M}_M$ and $\mathcal{M}_O$ are not accessible by this fitting procedure.

C. Local interfacial equilibrium vs complete reaction control

Boundary conditions corresponding to local equilibrium can be obtained by setting one or both of $\mathcal{M}_M$ and $\mathcal{M}_O$ to
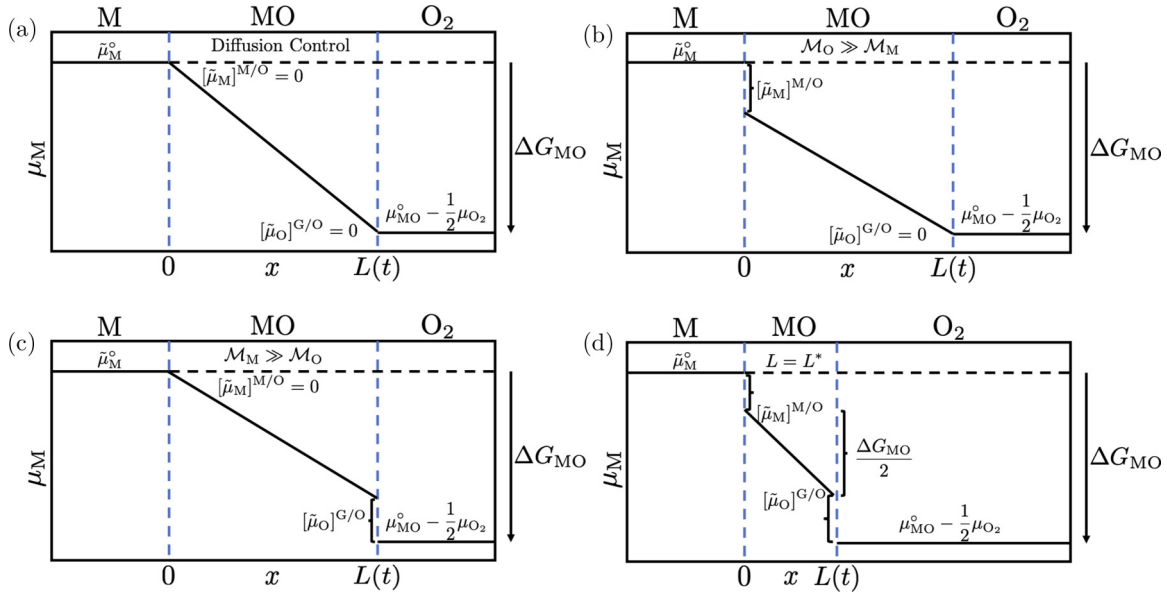
FIG. 4. An illustration of the distribution of the cation diffusion potential in the oxide for various limiting cases.

infinity since in this limit

$$\lim_{\mathcal{M}_M \to \infty} [\tilde{\mu}_M]^{M/O} = 0, \quad \lim_{\mathcal{M}_O \to \infty} [\tilde{\mu}_O]^{G/O} = 0, \quad (98)$$

which represents continuity of the diffusion potentials at the interfaces. If we choose $\mathcal{M}_M = \mathcal{M}_O = \infty$, the classical Wagner model of parabolic oxidation is obtained, and the film growth rate is given by Eq. (96). In this case, the driving force of the oxidation reaction is only dissipated by diffusion through the oxide. This is illustrated in Fig. 4(a), where it is clear that when $[\tilde{\mu}_M]^{M/O} = [\tilde{\mu}_O]^{G/O} = 0$, the entire diffusion potential change occurs in the oxide bulk, and diffusion within the oxide is the only process that dissipates free energy. This limit is also approached for thick films since from Eqs. (89) and (90):

$$\lim_{L \to \infty} [\tilde{\mu}_M]^{M/O} = \lim_{L \to \infty} [\tilde{\mu}_O]^{G/O} = 0. \quad (99)$$

This implies that diffusion will always become the rate limiting step once the film is sufficiently thick since the diffusion potential jumps go to zero and local equilibrium at the interfaces is established. This will occur regardless of the magnitude of ΔG_{MO}.

If local equilibrium is established only at one interface, then the driving force of the reaction is dissipated at the other interface and by diffusion through the oxide. When $\mathcal{M}_O \gg \mathcal{M}_M$, the gas-oxide interface is in local equilibrium, while the metal-oxide interface is out of equilibrium and a non-zero jump in the diffusion potential exists, as depicted in Fig. 4(b). In this case, the metal-oxide interface reaction is rate-limiting since the jump in the diffusion potential governs the magnitude of the fluxes. In the opposing limit of $\mathcal{M}_M \gg \mathcal{M}_O$, the metal-oxide interface is in local equilibrium while the gas-oxide interface is out of equilibrium, as shown in Fig. 4(c). In this case, the gas-oxide interface reaction is rate-limiting.

The presence of complete reaction control is difficult to determine experimentall, since it is possible to have a thickness-independent growth law and still have diffusion

dissipating the reaction free energy. Consider the instant where $L = L^*$, as shown in Fig. 4(d). In this case, the growth of the oxide is still linear in time and given by the equation

$$\frac{dL}{dt} = -\frac{\Omega^O \mathcal{M}_{\text{eff}}}{2} \Delta G_{MO.} \quad (100)$$

After some manipulation of the sum Eqs. (89) and (90), we find that at this film thickness

$$[\tilde{\mu}_O] + [\tilde{\mu}_M] = -\frac{\Delta G_{MO}}{2}. \quad (101)$$

This shows even for a thickness-independent growth law, the free energy dissipation is not necessarily confined to the interfaces. When $L = L^*$, half of the total reaction free energy change in dissipated at the oxide interfaces by the reactions, and the remaining half is dissipated by diffusion.

D. Defect behavior at the interfaces

Equations (89) and (90) yield expressions for the evolution of the interfacial vacancy concentrations as a function of the kinetic coefficients and oxide thickness. To illustrate, we assume an ideal solution model for the virtual chemical potentials that compose the potentials in the oxide [i.e., $\mu_i = \mu_i^\circ + RT \ln(c_i)$, where $c_i = \rho_i / \rho_s$ is the site fraction of species i in the oxide]. Considering the oxidation reaction $M + \frac{1}{2}O_2 \to MO + V_M$, the values of ΔG_{MO}° that can be read directly from an Ellingham diagram and the definition of ΔG_{MO} is given by the equation

$$\Delta G_{MO} = \Delta G_{MO}^\circ + RT \ln \left(P_{O_2}^{1/2} \right). \quad (102)$$

1. Gas-oxide interface

Inserting the virtual chemical potentials into Eq. (89), we find that the vacancy concentration at the gas-oxide interface is

$$c_{V_M''} = \frac{1}{4^{1/3}} \exp\left(-\frac{\Delta G_{G/O}^\circ - \alpha \Delta G_{MO}^\circ}{3RT} \right) P_{O_2}^{\frac{\alpha+1}{6}}, \quad (103)$$

where

$$\Delta G_{\text{G/O}}^{\circ} = \mu_{O_O^\times}^{\circ} + \mu_{V_M''}^{\circ} + 2\mu_{h^\bullet}^{\circ} - \frac{1}{2}\mu_{O_2}^{\circ}, \qquad (104)$$

which is the free energy change at the G/O interface in the standard state, and

$$\alpha = \frac{\mathcal{K}_{M_M^\times}}{\mathcal{M}_O(L + L^*)}. \qquad (105)$$

Equation (103) represents a generalization of the standard equilibrium mass action expression for the reaction $\frac{1}{2}O_2 \rightarrow O_O^\times + V_M'' + 2h^\bullet$ which predicts than $c_{V_M''}$ varies as $P_{O_2}^{1/6}$ at the gas-oxide interface. α is a new parameter that gives the fraction of ΔG_{MO} that is dissipated by the reaction at the gas-oxide interface. $\alpha = 0$ corresponds to local equilibrium, while $\alpha = 1$ corresponds to a 0 thickness film in the metal-oxide interface is in local equilibrium, an upper limit that is likely never reached in practice.

Since $\alpha \geqslant 0$ and $\Delta G_{\text{MO}}^{\circ} < 0$, we can see that when finite reaction kinetics are taken into account, the vacancy concentration at the gas-oxide interface is lower than its value at equilibrium, assuming that the pressure is fixed. As the film grows, α decreases to zero and the usual mass action expression and $P_{O_2}^{1/6}$ pressure dependence is recovered. Thus, when there is interfacial nonequilibrium, the exponent of the pressure dependence of the vacancy concentration will change from its standard value.

2. Metal-oxide interface

Inserting the virtual chemical potentials into Eq. (90), we obtain the following nonlinear equation for the vacancy concentration at the metal-oxide interface

$$\frac{c_{V_M''}^3}{\left(1 - c_{V_M''}\right)} = \frac{1 - c_M}{4c_M} \exp\left(\frac{\Delta G_{\text{M/O}}^{\circ} - \beta\Delta G_{\text{MO}}^{\circ}}{RT}\right) P_{O_2}^{-\frac{\beta}{2}}. \quad (106)$$

Since we assumed throughout the derivation that c_{V_M} is small, Eq. (106) becomes,

$$c_{V_M''} \approx \left(\frac{1 - c_M}{4c_M}\right)^{1/3} \exp\left(\frac{\Delta G_{\text{M/O}}^{\circ} - \beta\Delta G_{\text{MO}}^{\circ}}{3RT}\right) P_{O_2}^{-\frac{\beta}{6}}, \quad (107)$$

where

$$\Delta G_{\text{M/O}}^{\circ} = \mu_{M_M^\times}^{\circ} + \mu_{V_M}^{\circ} - \mu_M^{\circ} - \mu_{V_M''}^{\circ} - 2\mu_{h^\bullet}^{\circ} \qquad (108)$$

is the change in free energy at the metal-oxide interface in the standard state, and

$$\beta = \frac{\mathcal{K}_{M_M^\times}}{\mathcal{M}_M(L + L^*)}. \qquad (109)$$

Similar to α, β is a parameter that defines the fraction of the net reaction ΔG that is dissipated at the metal-oxide interface and $0 \leqslant \beta \leqslant 1$. Again, $\beta = 0$ corresponds to local-equilibrium of the metal-oxide interface. $\beta = 1$ corresponds to a 0 thickness film and local equilibrium of a the gas-oxide interface, a limit that is likely not reached in practice.

For nonzero β, the exponential term leads to an increase in the vacancy concentration, while the pressure dependence leads to a decrease in the vacancy concentration with respect to the equilibrium value when $\beta = 0$. As a film thickens and

β evolves toward 0, the vacancy concentration relaxes to its equilibrium value that is independent of P_{O_2}. Since the net driving force, ΔG_{MO} for oxidation is on the order -10^5 J/mol, and P_{O_2} is typically less than 1 bar, we believe that the exponential term will dominate and a vacancy supersaturation is present at the metal-oxide interface for sufficiently thin films when β is nonzero.

Plots of the defect concentrations at the interfaces as a function of the kinetic parameters α and β and P_{O_2} are shown in Fig. 5. When kinetic effects are taken into account, we can see that for thin films, the deviations from local equilibrium at the interfaces lead to a vacancy excess at the metal-oxide interface and a vacancy deficit at the gas-oxide interface compared to local equilibrium when $\alpha, \beta = 0$. When interfacial kinetics are taken into account, there is a P_{O_2} dependence to the vacancy concentration at the metal-oxide interface, despite the fact that that interface is isolated from the gas-phase and oxygen gas is not a participant in the metal-oxide interface reaction given by Eq. (71). As the film grows and α and β decrease to 0, the equilibrium results are recovered and, in particular, the pressure dependence of the vacancy concentration at the metal-oxide interface disappears as expected.

We note that a possible implication of the nonequilibrium vacancy supersaturation at the metal-oxide interface is the formation of voids in the oxide at that interface. Voiding in thin oxide films has been noted by Xu *et al.*, which they explained as a result of stress gradient driving vacancy coalescence in the oxide [20]. We propose an alternate explanation which is that since the oxides in their analysis are thin (10 nm) or less, that the voids are the result of the vacancy supersaturation present under nonequilibrium conditions. If the vacancies are present in high-enough concentrations, they can coalesce to form these voids.

Considering the implications of Eqs. (103) and (107), we can see that for a sufficiently thin film ($L \approx L^*$), the effect of increasing P_{O_2} is to increase the vacancy concentration at the gas-oxide interface while simultaneously decreasing the vacancy concentration at the metal-oxide interface. The combined effect is an increased vacancy flux across the film and thus an increase in the growth rate of the film. This is consistent with observation of faster film growth kinetics as P_{O_2} increases [3].

As another illustration of how a deviation from local equilibrium impacts the behavior of the vacancy concentrations at the metal-oxide and gas-oxide interfaces, we plot $\ln(c_{V_M''})$ vs $\ln(P_{O_2})$ in Fig. 6, for various values of α and β. As shown in Fig. 6(a), when local equilibrium is established at the gas-oxide interface ($\alpha = 0$) the slope of the plot is 1/6 which indicates a $P_{O_2}^{1/6}$ dependence, which is usual exponent found in the literature on rocksalt oxides. As α is increased from 0 and the departure from equilibrium is larger, the slope increases and is always equal to $(\alpha + 1)/6$. Thus if the film is thin such that these nonequilibrium effects are important, the measured exponent of the pressure dependence of the vacancy concentration at the gas-oxide interface can range from $1/6 - 1/3$.

In Fig. 6(b), we show the same plot at the metal-oxide interface. Here, in local equilibrium ($\beta = 0$, the defect concentration is independent of the oxygen pressure (slope is 0), which follows from the fact that oxygen gas is not
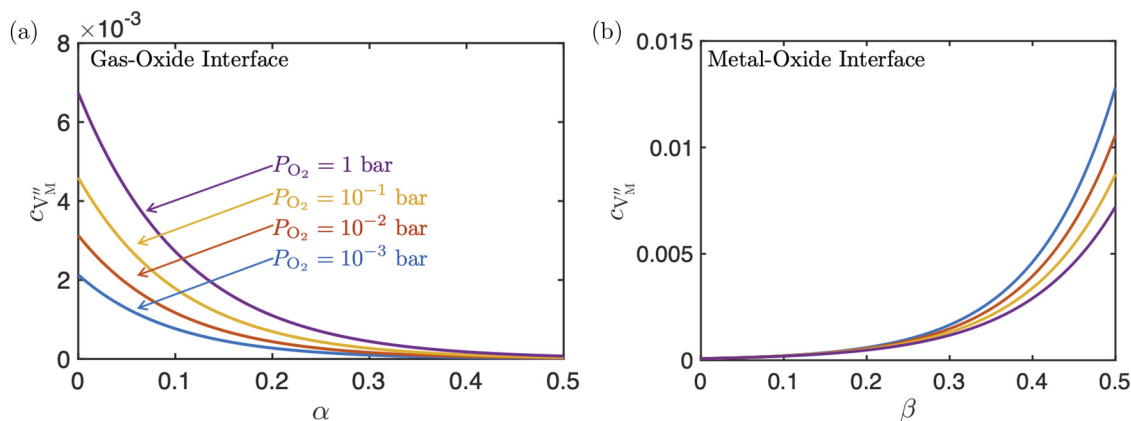
FIG. 5. Plots of the defect concentrations at the (a) gas-oxide and (b) metal-oxide interfaces as a function of the kinetic parameters α and β and P_{O_2} for $T = 773.15$ K. $\Delta G^{\circ}_{MO} = -175$ kJ/mol, $\Delta G^{\circ}_{G/O} = -\Delta G^{\circ}_{MO}/2$, and $\Delta G^{\circ}_{M/O} = 3\Delta G^{\circ}_{MO}/2$. The same O_2 pressures are used in both (a) and (b).

a participant in the metal-oxide interface reaction. As the deviation from local equilibrium is increased, the slope becomes nonzero and the exponent of the P_{O_2} dependence of the vacancy concentration is nonzero and is equal to $-\beta/6$. Therefore, if the film is sufficiently thin, the exponent can vary from $-1/6 - 0$.

VI. SUMMARY AND FUTURE WORK

We applied irreversible thermodynamics to derive a general model for the high-temperature oxidation of a metal in which local interfacial equilibrium is not necessarily maintained. The resulting dissipation rate accounts for bulk and interfacial processes, including capillary contributions to the interface shape evolution. We examine the implications of the model for oxide growth in one dimension, and find that the general solution captures the transition from linear to parabolic kinetics and the relaxation to local interfacial equilibrium as the film grows. We show that the Wagner model can be obtained

as a limiting case of our general model when the mobilities of atoms across the interfaces of the metal-oxide and oxide-gas interfaces are infinite, or when the film thickness approaches infinity. We identify a characteristic thickness for the transition from linear to parabolic kinetics that is given by the ratio of the bulk mobility of cations in the oxide film $\mathcal{K}_{M_M^{\times}}$ to an effective interfacial mobility of atoms $\mathcal{M}_{\text{eff}}$ which accounts for reactions occurring simultaneously at the metal-oxide and gas-oxide interfaces. We show that by fitting our growth law to measurements of the oxide film thickness as a function of time can determine the values of the coefficients $\mathcal{K}_{M_M^{\times}}$ and $\mathcal{M}_{\text{eff}}$. For small film thicknesses and interfacial mobilities, we find that the vacancy concentrations at the interfaces deviate from the equilibrium values and importantly, find that a vacancy supersaturation is present at the metal-oxide interface. We also show that when the oxide is thin such that these nonequilibrium effects are important, the exponents for the pressure pressure dependence of the oxygen vacancy concentrations at the gas-oxide and metal-oxide interfaces with deviate from the equilibrium values of 0 and 1/6.
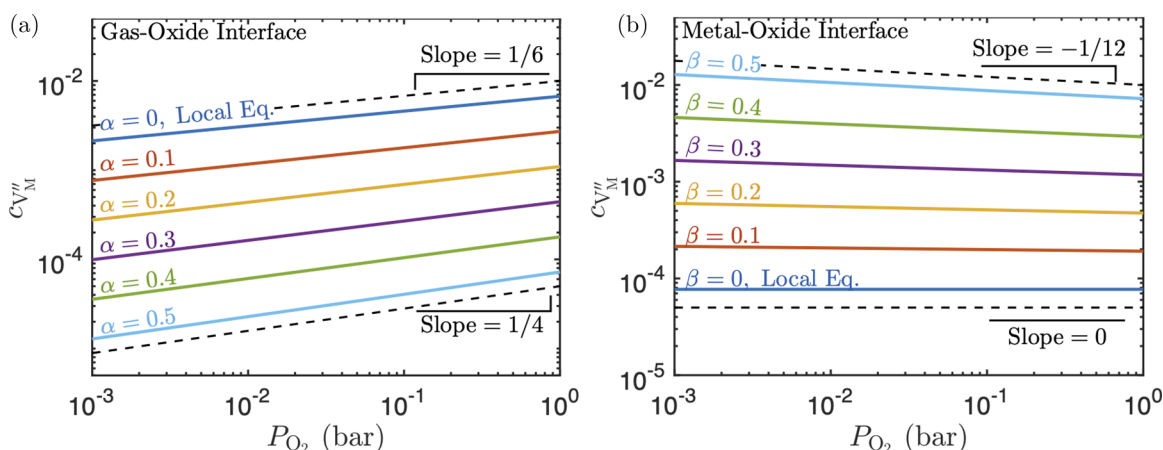

FIG. 6. Plots of $\ln(c_{V_M''})$ versus $\ln(P_{O_2})$ for various values of the kinetic parameters α and β. Panel (a) shows the vacancy concentration at the gas-oxide interface and (b) shows the vacancy concentration at the metal-oxide interface. The plots shows how the exponent for the P_{O_2} dependence deviates from the predicted exponents from reaction equilibrium arguments as α and β increase from 0, which corresponds to local equilibrium.

The approach to oxidation modeling developed here serves as an important first step to describing the phenomenon of solute capture during high temperature oxidation of single-phase alloys which has recently been reported [17]. In these experiments, Ni-Cr alloys were oxidized at high temperature resulting a single solid-solution rocksalt oxide containing Cr in concentrations that far exceed the equilibrium solubility of Cr in NiO. A departure from local equilibrium at the metal-oxide interface is necessary for such oxides to form, and the framework for including nonequilibrium interfaces described here provides a basis for modeling this process. Subsequent work will involve extending the model derived here to multi-component alloys and oxides to describe solute capture.

[1] A. Atkinson, Rev. Mod. Phys. **57**, 437 (1985).

[2] H. Schmalzried, *Chemical Kinetics of Solids* (VCH Verlagsgesellschaft mbH, Weinheim, 1995).

[3] J. Young, *High Temperature Oxidation and Corrosion of Metals*, Vol. 1 (Elsevier, Amsterdam, 2008), pp. 81–137.

[4] C. Wagner, Z. Phys. Chem. **21B**, 25 (1933).

[5] C. Y. Chao, J. Electrochem. Soc. **128**, 1187 (1981).

[6] A. Couet, A. T. Motta, and A. Ambard, Corros. Sci. **100**, 73 (2015).

[7] C. Wagner, Corros. Sci. **9**, 91 (1969).

[8] D. J. Young and F. Gesmundo, Oxid. Met. **29**, 169 (1988).

[9] W. C. Johnson, Metall. Mater. Trans. A **29**, 2021 (1998).

[10] M. E. Gurtin and P. W. Voorhees, Acta Mater. **44**, 235 (1996).

[11] R. Grace and T. Kassner, Acta Metall. Mater. **18**, 247 (1970).

[12] F. S. Pettit and J. B. Wagner, Acta Metall. Mater. **12**, 35 (1964).

[13] D. D. MacDonald, S. R. Biaggio, and H. Song, J. Electrochem. Soc. **139**, 170 (1992).

[14] C. Wagner, Berich. Bunsen. Gesell. **70**, 775 (1966).

[15] Y. Unutulmazsoy, R. Merkle, D. Fischer, J. Mannhart, and J. Maier, Phys. Chem. Chem. Phys. **19**, 9045 (2017).

[16] Y. Mishin, G. B. McFadden, R. F. Sekerka, and W. J. Boettinger, Phys. Rev. B **92**, 064113 (2015).

[17] X. X. Yu, A. Gulec, Q. Sherman, K. L. Cwalina, J. R. Scully, J. H. Perepezko, P. W. Voorhees, and L. D. Marks, Phys. Rev. Lett. **121**, 145701 (2018).

[18] M. H. Lankhorst, H. J. Bouwmeester, and H. Verweij, J. Am. Ceram. Soc. **80**, 2175 (1997).

[19] S. Perusin, B. Viguier, D. Monceau, L. Ressier, and E. Andrieu, Acta Mater. **52**, 5375 (2004).

[20] X. X. Yu, A. Gulec, C. M. Andolina, E. J. Zeitchick, K. Gusieva, J. C. Yang, J. R. Scully, J. H. Perepezko, and L. D. Marks, Corrosion **74**, 939 (2018).